(Invitrogen) according to the manufacturer's instructions. Amounts of RNA per unit cell number (18.3 ± 0.6 μg vs. 22.8 ± 4.5 μg, $P < 0.349$) from non-SCI and SCI mice did not differ significantly from each other when the same number of BM cells (2×10^7 cells) was compared. Appendix Figure 1 shows the amounts of total RNA from non-SCI and SCI mice extracted separately. All reactions were performed in triplicate. Then, total RNA extracted from non-SCI and SCI mice at the same amounts was transcribed with avian reverse transcriptase, Superscript (Life Technologies) and Oligo-dT primer (Promega). RT products were inactivated at 98°C for 10 min with a heat block, followed by quantitative real-time PCR performed using the TaqMan universal PCR master mix (Applied Biosystems) and specific primers and probes, with the Applied Biosystems 7900 sequence detection system, version 2.0. Specific primers and probes for GAPDH were purchased from Applied Biosystems (TaqMan Mm99999915_g1). PCR conditions and data analysis were performed according to the instructions in the sequence detection system, version 2.0.

Appendix Figure 2 shows the ratio of expression of GAPDH from senescent SCI mice expressed as those from non-SCI mice (three mice each) considered as 1.0. Both expressions were not significantly different from each other (1.0 vs. 1.3, respectively, $P < 0.2316$).

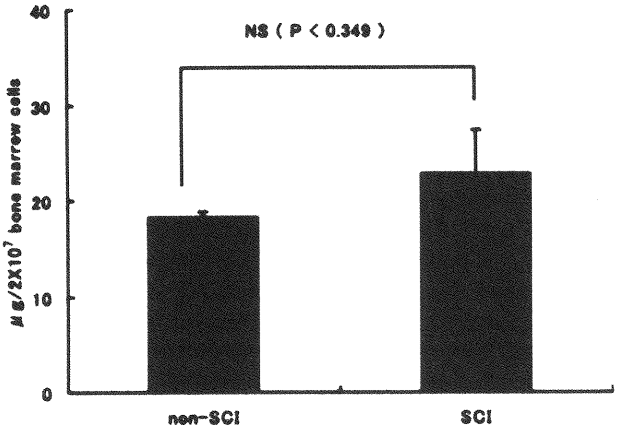

Appendix Figure 1. Relative amounts of RNA per unit cell number from non-SCI and SCI mice. Total RNA was extracted from the same number of BM cells (2×10^7) from the non-SCI and SCI mice using TRIzol (Invitrogen). Each bar represents the mean ± SD obtained from triplicate experiments.

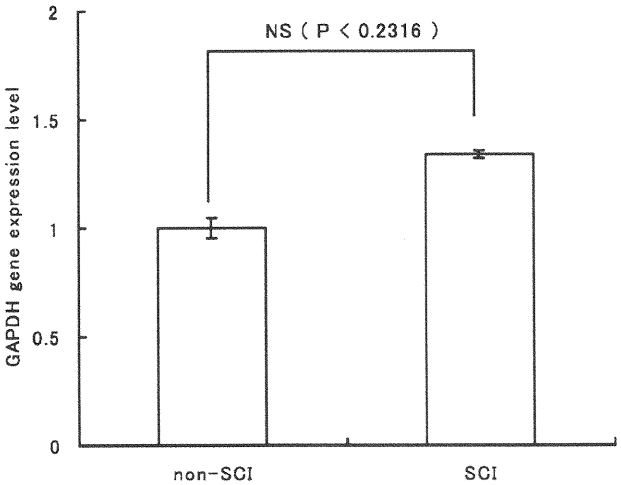

Appendix Figure 2. Relative expression levels of GAPDH from non-SCI and SCI mice. RNA extracted from non-SCI mice and SCI mice at the same amount was reverse-transcribed using Superscript (Life Technologies) and Oligo-dT(Promega). The reverse-transcribed complementary DNAs were then amplified by real-time polymerase chain reaction using TaqMan PCR master mix (Applied Biosystems) and specific primer for murine GAPDH. Each bar represents the mean ± SD obtained from triplicate experiments.

1. Rembold H, Gyure WL. Biochemistry of the pteridines. Angew Chem Int Ed Engl 11:1061–1072, 1972.
2. Huber C, Batchelor JR, Fuchs D, Hausen A, Lang A, Niederwieser D, Reibnegger G, Swetly P, Troppmair J, Wachter N. Immune response-associated production of neopterin. Release from macrophages primarily under control of interferon-gamma. J Exp Med 160:310–316, 1984.
3. Niederwieser D, Huber C, Gratwohl A, Bannert P, Fuchs D, Hausen A, Reinbnegger G, Speck B, Wachter H. Neopterin as a new biochemical marker in the clinical monitoring of bone marrow transplant recipients. Transplantation 38:497–500, 1984.
4. Reibnegger G, Aulitzky W, Huber C, Margreoter R, Riccabona G, Wachter H. Neopterin in urine and serum of renal allograft recipients. J Clin Chem Biochem 24:770–775, 1986.
5. Schobersberger W, Hoffmann G, Hobisch-Hagen P, Bock G, Volkl H, Baier-Bitterlich G, Wirleitner B, Wachter H, Fuchs D. Neopterin and 7,8-dihydroneopterin induce apoptosis in the rat alveolar epithelial cell line L2. FEBS Lett 397:263–268, 1996.
6. Kojima S, Nomura T, Icho T, Kajiwara Y, Kitabatake K, Kubota K. Inhibitory effect of neopterin on NADPH-dependent superoxide-generating oxidase of rat peritoneal macrophages. FEBS Lett 329: 125–128, 1993.
7. Schobersberger W, Jelkmann W, Fandrey J, Frede S, Wachter H, Fuchs D. Neopterin-induced suppression of erythropoietin production *in vitro*. Pteridines 6:12–16, 1995.
8. Uberall F, Werner-Felmayer G, Schubert C, Grunicke HH, Wachter H, Fuchs D. Neopterin derivatives together with cyclic guanosine monophosphate induce c-*fos* gene expression. FEBS Lett 352:11–14, 1994.
9. Schobersberger W, Hoffmann G, Grote J, Wachter H, Fuchs D. Induction of inducible nitric oxide synthase expression by neopterin in vascular smooth muscle cells. FEBS Lett 377:461–464, 1995.
10. Kibourn RG, Traber DL, Szabo C. Nitric oxide and shock. Dis Mon 43: 277–348, 1997.
11. Aizawa S, Hiramoto M, Araki S, Negishi S, Kimura Y, Hoshi G, Kojima S, Wakasugi K. Stimulatory effects of neopterin on hematopoiesis *in vitro* are mediated by activation of stromal-cell function. Hematol Oncol 16:57–67, 1998.
12. Aizawa S, Hamamoto H, Araki S, Hoshi H, Kojima S, Wakasugi K. *In vivo* stimulatory effects of neopterin on hematopoiesis. Pteridines 9:13–17, 1998.
13. Takeda T, Hosokawa M, Takeshita S, Irino M, Higuchi K, Matsushita T, Tomita Y, Yasuhira K, Hamamoto H, Shimizu K, Ishii M, Yamamuro T. A new murine model of accelerated senescence. Mech Ageing Dev 17:183–194, 1981.
14. Izumi-Hisha H, Ito Y, Sugimoto K, Oshima H, Mori KJ. Age-related decrease in the number of hemopoietic stem cells and progenitors in senescence accelerated mice. Mech Ageing Dev 56:89–97, 1990.

15. Tsuboi I, Morimoto K, Horie T, Mori KJ. Age-related changes in various hemopoietic progenitor cells in senescence-accelerated (SAM-P) mice. Exp Hematol 19:874–877, 1991.
16. Tsuboi I, Morimoto K, Hirabayashi Y, Li GX, Aizawa S, Mori KJ, Kanno J, Inoue T. Senescent B lymphopoiesis is balanced in suppressive homeostasis: decrease in interleukin-7 and transforming growth factor-β levels in stromal-cells of senescence-accelerated mice. Exp Biol Med (Maywood) 229:494–502, 2004.
17. Riley RL, Kruger MG, Elia J. B cell precursors are decreased in senescent BALB/c mice, but retain normal mitotic activity *in vivo* and *in vitro*. Clin Immunol Immunopathol 59:301–313, 1991.
18. Fuchs D, Stahl-Hennig C, Gruber A, Murr C, Hunsmann G, Wachter H. Neopterin—its clinical use in urinalysis. Kidney Int Suppl 47:S8–S11, 1994.
19. Nagaoka H, Gonzalez-Aseguinolaza G, Tsuji M, Nussenzweig MC. Immunization and infection change the number of recombination activating gene (RAG)-expressing B cells in the periphery by altering immature lymphocyte production. J Exp Med 191:2113–2120, 2000.
20. Ueda Y, Yang K, Foster SJ, Kondo M, Kelsoe G. Inflammation controls B lymphopoiesis by regulating chemokine CXCL12 expression. J Exp Med 199:47–58, 2004.
21. Ueda Y, Kondo M, Kelsoe G. Inflammation and the reciprocal production of granulocytes and lymphocytes in bone marrow. J Exp Med 201:1771–1780, 2005.
22. Wirleitner B, Obermoser G, Bock G, Neurauter G, Schennach H, Sepp N, Fuchs D. Induction of apoptosis in human blood T cells by 7,8-dihydroneopterin: the difference between healthy controls and patients with systemic lupus erythematosus. Clin Immunol 107:152–159, 2003.
23. Nemunaitis J, Tompkins CK, Andrews DF, Singer JW. Transforming growth factor beta expression in human marrow stromal-cells. Eur J Haematol 46:140–145, 1991.
24. Hoffman G, Schobersberger W, Frede S, Pelzer L, Fandrey J, Wachter H, Fuchs D, Grote J. Neopterin activates transcription factor nuclear factor-κB in vascular smooth muscle cells FEBS Lett 391:181–184, 1996.
25. Hoffman G, Kenn S, Wirleitner B, Deetjen C, Trede S, Smolny M, Rieder J, Fuchs D, Baier-Bitterlich G, Schobersberger W. Neopterin induces nitric oxide-dependent apoptosis in rat vascular smooth muscle cells. Immunobiol 199:63–73, 1998.
26. Lee G, Namen AE, Gillis S, Ellingsworth LR, Kincade PW. Normal B cell precursors responsive to recombinant murine IL-7 and inhibition of IL-7 activity by transforming growth factor-beta. J Immunol 142:3875–3883, 1989.
27. Fernandez S, Knopf MA, Shankar G, McGillis JP. Calcitonin gene-related peptide indirectly inhibits IL-7 responses in pre-B cells by induction of IL-6 and TNF-alpha in bone marrow. Cell Immunol 226: 67–77, 2003.
28. Barak M, Gruener N. Neopterin augmentation of tumor necrosis factor production. Immunol Lett 30:101–106, 1991.
29. Hoffmann G, Frede S, Kenn S, Smolny M, Wachter H, Fuchs D, Grote J, Rieder J, Schobersberger W. Neopterin-induced tumor necrosis factor-alpha synthesis in vascular smooth muscle cells *in vitro*. Int Arch Allergy Immunol 116:240–245, 1998.
30. Nakamura K, Kouro T, Kincade PW, Malykhin A, Maeda K, Coggeshall KM. Src homology 2-containing 5-inositol phosphatase (SHIP) suppresses an early stage of lymphoid cell development through elevated interleukin-6 production by myeloid cells in bone marrow. J Exp Med 199:243–254, 2004.
31. Maeda K, Baba Y, Nagai Y, Miyazaki K, Malykhin A, Nakamura K, Kincade PW, Sakaguchi N, Coggeshall KM. IL-6 blocks a discrete early step in lymphopoiesis. Blood 106:879–885, 2005.
32. Saito H, Sherwood ER, Varma TK, Evers BM. Effect of aging on mortality, hypothermia, and cytokine induction in mice with endotoxemia or sepsis. Mech Ageing Dev 124:1047–1058, 2003.
33. Tateda K, Matsumoto T, Miyazaki S, Yamaguchi K. Lipopolysaccharide-induced lethality and cytokine production in aged mice. Infect Immun 64:769–774, 1996.

ELSEVIER

EXPERIMENTAL HEMATOLOGY

Experimental Hematology 35 (2007) 125–133

Implications of hemopoietic progenitor cell kinetics and experimental leukemogenesis: Relevance to Gompertzean mortality as possible hematotoxicological endpoint

Yoko Hirabayashi[a] and Tohru Inoue[b]

[a]*Cellular and Molecular Toxicology Division, Center for Biological Safety and Research, National Institute of Health Sciences, Tokyo, Japan;* [b]*Center for Biological Safety and Research, National Institute of Health Sciences, Tokyo, Japan*

Objective. **The aim of this study is to investigate a possible implication in cell kinetics of the hematopoietic progenitors to the experimental leukemogenesis to elucidate the relevance of various leukemic mode of action to Gompertzean survival curves, a new parameter based on the lifespan.**

Materials and Methods. **Mice, C3H/He, and C57BL/6 strain, male and female, with or without genetic modifications, e.g., p53-deficiency or thioredoxin overexpression were used in the present hemopoietic stem/progenitor research, radiation- or benzene-induced leukemogenesis followed by histopathological examination. A lethal dose of radiation for bone marrow transplantation, and a graded increased dose up to 5 Gy of x-rays for induction of hematopoietic malignancies were given. For caloric restriction studies, 77 kcal/week was maintained in accordance to different restriction-timing. For assays of hematopoietic colonization, colony-forming unit spleen and colony-forming unit granulocyte macrophage were evaluated. Hematopoietic progenitor cell-specific kinetics were studied by continuous labeling of bromodeoxyuridine for cycling cells, followed by ultraviolet (UV) exposure and hemopoietic colonization (bromodeoxyuridine UV [BUUV] method). Various experimental survival curves were applied to a mathematical analysis by Gompertz-Makeham law of mortality.**

Results. **Referring current authors' studies on leukemogenesis induced by ionizing radiation and benzene exposure, implications of hematopoietic progenitor cell kinetics to the experimental leukemogenesis were evaluated by means of a novel experimental tool, the BUUV method. Comparative studies to elucidate relevancies of these data, including two prevention studies, one on caloric restriction and the other on antioxidative thioredoxin overexpression, to those Gompertzean survival curves of experimental animals were analyzed.**

Conclusion. **The Gompertzean expression may elucidate an appropriate toxicological endpoint for evaluating the effect of radiation and/or benzene-exposure on the lifespan and its modification by various experimental preventive measures.** © **2007 International Society for Experimental Hematology. Published by Elsevier Inc.**

The principle of the mortality rate of human beings was recognized by Gompertz [1] more than 180 years ago, who described that mortality rate during a unit time interval increases exponentially with lifetime. It was found that the Gompertzean expression can be applied to major mammalian species, and that the slope of the Gompertzean curve becomes shallower along the evolutionary hierarchy of the animal kingdom from rodents to humans. Moreover, when one applies the Gompertzean expression to a particular species, e.g., mice, one could note that regardless of type of compound, whether carcinogenic compounds or other life-threatening chemical compounds, the slope is steeper, indicating a shortening of lifespan not only attributable to carcinogenic impact but also cardiovascular, nephrotoxic, and other nontumorigenic diseases.

Radiation and benzene are the ultimate human leukemogens, known for over eight decades, on which the late Eugene P. Cronkite focused his attention and which he used to compare mechanisms of toxicities induced by radiation and benzene exposure [2,3]. His most notable strategy in studying mechanisms underlying leukemogenesis induced by

Offprint requests to: Yoko Hirabayashi, M.D., Ph.D., Cellular and Molecular Toxicology Division, Center for Biological Safety and Research, National Institute of Health Sciences, 1-18-1 Kamiyohga, Setagayaku, Tokyo 158-8501, Japan; E-mail: yokohira@nihs.go.jp

0301-472X/07 $–see front matter.
doi: 10.1016/j.exphem.2007.01.020

both compounds was to focus on the relevancy of the number and quality of hemopoietic stem/progenitor cells and their significance in stem/progenitor cell kinetics in relation to leukemogenicity. Because an increase in radiation dose exponentially decreases the number of hemopoietic progenitor cells (Fig. 1A, line "a"), exposure to an ionizing radiation of >5 Gy will not yield a high frequency of leukemias, but will induce a significant decrease in the incidence of leukemias, possibly because of the decrease in the number of hemopoietic progenitor cells (although it remains unclear whether stem/progenitor cells are leukemic target cells). The minimum number of potentially mutated stem/progenitor cells for the development of one case of leukemia decreases with increase in radiation dose (Fig. 1A, line "b"). Thus, the integral of the shaded area shown in Figure 1 between those two functions may correlate to the risk of radiation-induced leukemias, although the scale of the ordinate for the stem/progenitor cell survival curve described here may be arbitrary. Namely, the shaded shared area between the area beneath the stem/progenitor cell survival curve and the upper area of the lower curve, i.e., the minimum number of mutated stem/progenitor cells for the development of one case of leukemia as a function of radiation dose, may be the risk factor for radiation-induced leukemogenesis. Furthermore, when one incorporates corresponding data from p53-knockout mice (Fig. 1B) and other data from genetically modified animals, any modifications of shared areas suggest a decrease and/or an increase in risk of the incidence of experimental leukemogenesis. Such statistical relevance between the number of hemopoietic stem/progenitor cells and the induction of experimental leukemias can be applied also to the study of the incidence of benzene-induced leukemias. In the case of benzene-induced leukemias, the relevance of stem cell kinetics to the incidence of experimental leukemias is a function of changes in hemopoietic progenitor cells. In this article, such relevancies between the number and quality of stem/progenitor cells and the incidence of leukemias after radiation and/or benzene exposure with respect to biological modification after caloric restriction and/or modification of the state of oxidative stress are introduced after a brief description of the characteristics of hemopoietic progenitor cell function.

Materials and methods

Mice

C3H/He and C57BL/6 strain, male and female, with or without genetic modification for p53 deficiency [4] or thioredoxin overexpression [5] were used in the hemopoietic stem/progenitor cell research, radiation- or benzene-induced leukemogenesis followed by histopathological examination. Experimental animal protocols used were reviewed by the externally established peer-review panel, and maintained in the board-approved laboratory animal facility of the National Institute of Health Sciences of Japan.

Radiation and bone marrow transplantation

For a lethal dose of radiation (9.45 Gy) for bone marrow transplantation and a graded increased dose up to 5.0 Gy of x-ray irradiation for induction of hematopoietic malignancies, mice were subjected to a 200-kV/20 A pulse through a therapeutic x-ray irradiator (Shimadzu, Tokyo) with 1.0-mm aluminum and 0.6-mm copper filters, at a dose rate of 0.614 Gy/minute and a 56-cm focus surface distance. Whole-body irradiation (8.5 Gy) by gamma-ray

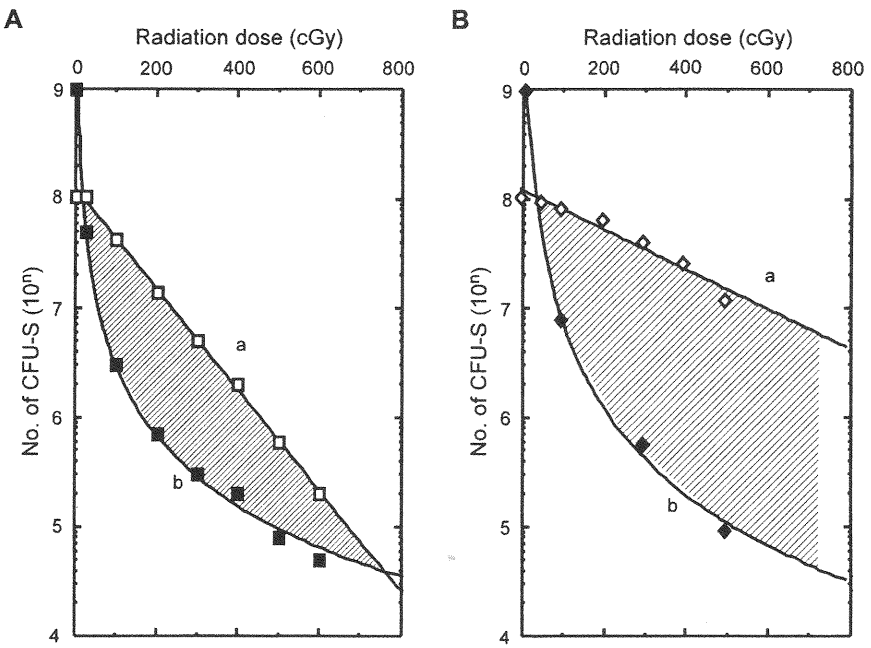

Figure 1. Possible risk of radiation-induced leukemia in wild-type mice (**A**) and p53-homozygous knockout mice (**B**). (**a**) Survival of stem cells after irradiation. (**b**) Minimum number of stem cells for development of a case of leukemia.

(^{137}Cs, at a dose rate of 0.101 Gy/minute, Gammacell 40 Exactor; MDS Nordion, Ottawa, Canada) with a 0.5-mm aluminum-copper filter was also given in the assay of colony-forming unit in spleen.

Benzene and benzene exposure

Benzene (CAS no. 71-43-2, MW 78.11) was purchased from Wako Fine Chemical Company (Osaka, Japan). Mice were randomly assigned to groups and individually housed. They were exposed to benzene in 1.3 m^3 inhalation chambers as described previously [6,7]. The benzene-exposed mice were exposed to 300 ppm of benzene 6 hours per day, 5 days per week for 2 weeks for short-term examination, and 26 weeks for leukemogenicity bioassay. The mice were supplied water ad libitum, but food pellets were withdrawn during the exposure.

Caloric restriction

For caloric restriction studies, a 77 kcal/week was maintained. Groups subjected to different caloric restriction timings were compared with groups not subjected to caloric restriction during lifetime for incidences of neoplasms followed by histopathological examination [8,9].

Assays for CFU-S and CFU-GM

For assay of hematopoietic colonization, colony-forming unit in spleen (CFU-S) [10] and colony-forming unit granulocyte macrophages (CFU-GM) [7,11] were evaluated. For CFU-GM assay, a semisolid methylcellulose culture, supplemented with 10 ng/mL murine granulocyte macrophage colony-stimulating factor (R&D Systems, Inc., Minneapolis, MN, USA) was conducted.

BUUV method

Hematopoietic progenitor cell-specific kinetic studies were evaluated by continuous labeling of bromodeoxyuridine for cycling cells, followed by UV exposure and hemopoietic colonization (BUUV method, details in [11,12]).

Gompertzean expression

Experimental survival curves were applied to Gompertz's law of mortality to examine lifespans and mortality rates in mice with ionizing radiation- and benzene-induced leukemias. (Detailed procedure of mathematical analysis by Gompertz-Makeham law of mortality is found in ref. [1].).

Results and discussion

Hemopoietic stem/progenitor cells as a target of experimental leukemogenesis

Because the major histopathological type of radiation-induced leukemia in p53-deficient mice was stem cell leukemia with trace evidence of myeloid differentiation, the possible target cells in leukemogenesis were supposed to be hemopoietic stem/progenitor cells [13]. Interestingly, p53-heterozygous deficiency also produced stem cell leukemia with loss of heterozygousity after graded increased doses of radiation exposure (unpublished observation). Therefore, to understand the mechanism underlying leukemogenesis induced by radiation and/or benzene exposure, current series of evidence regarding stem/progenitor cell characteristics are particularly important. Furthermore, in addition to the generation-age structure of hierarchic stem/progenitor cells, current knowledge on genes regulating kinetics in stem/progenitor cells (i.e., genes maintaining the long-term repopulating cells), genes in splenic colony-forming units, and genes in in vitro colony-forming units, is found to be particularly important for understanding development of leukemias. Because of the possible participation of negative regulators of stem/progenitor cell differentiation and self-renewal, such as *Notch* [14], *Wnt* [15], and *Sonic hedgehog* [16] signals, and *Bmi-1* [17] expression, a dormant fraction, about 80% in the hemopoietic stem/progenitor cell compartment, which does not incorporate bromodeoxyuridine (BrdUrd), is continuously maintained for lifetime after the development of this dormant fraction during the neonatal stage. The cycling fraction, on the other hand, incorporates BrdUrd continuously and about 20% of the total progenitor cell compartment is maintained throughout the lifespan. Furthermore, the doubling time of each progenitor cell compartment in the stem/progenitor hierarchy is facilitated in the order from immature progenitor cells with faster generation time to mature progenitor cells with slower generation time (data not shown). The size of dormant fractions slightly decreases with the age structure of progenitor cells. We previously observed that hemopoietic progenitor cells also maintain their immaturity with transforming growth factor-β (TGF-β) [18], as well as gap junctional intercellular communication, specifically with connexin-32, which was supposed to maintain the size of the immature stem/progenitor cell compartment, steady-state growth, regenerating potential after experimental chemical abrasion, and possibly function as a tumor suppressor for leukemogenesis.

Novel tool to evaluate hemopoietic progenitor-specific cell kinetics (BUUV method[1]) as a key parameter for leukemogenesis

The concept of a stem/progenitor cell pool and the daily outflow (i.e., production) of committed cells to erythropoietic, granulopoietic, and megakaryocytic lineages were also intensively studied by Cronkite and his associates from the 1960s to the 1970s. They determined the number of stem/progenitor cells undergoing DNA synthesis using tritiated thymidine (^{3}H-TdR) with a low specific radioactivity as well as the incorporation of ^{3}H-TdR with a cytocidal dose of high-specific activity for evaluating the cycling fraction [19]. In the early 1980s, Cronkite applied his knowledge on steady-state hematopoiesis to toxicological studies, not only to the radiation-induced, but also benzene-induced, hemopoietic toxicities and their consequence, namely,

[1]Continuous infusion of bromodeoxyuridine by osmotic minipump to label cycling cells in general is carried out, followed by UV exposure to kill labeled cells, and then allowing surviving stem cells to form hemopoietic colonies.

leukemogenesis [20]. Cell kinetic studies using ^{3}H-TdR with low- and high-specific activities provided a new paradigm of benzene- and other chemical-related hematotoxicities.

There are two technical limitations of the experimental and hematological use of ^{3}H-TdR. First, ^{3}H-TdR with a low-specific activity enables labeling of cycling cells, but not killing them, second, ^{3}H-TdR with a high-specific activity, enables the labeling and killing of cycling cells, but not the studying of long-term cell kinetics. The BUUV method established by Hirabayashi and coworkers [11,12] entails the purging of cells labeled by BrdUrd using UV-A light for evaluating the kinetics of hemopoietic progenitor cells, followed by colonization and other hematological evaluations (Fig. 2). The method enables long-term labeling of cycling cells for up to nearly a lifetime and the assay of the size of the cytocide fraction at anytime by exposure to UV-A light followed by relevant colonization assay methods and/or cell sorting. Although many similar methods were reported previously, none of them are appropriate for hemopoietic stem cell research. The reasons are as follows: In previous methods, UV-B and UV-C lights were used, not UV-A light, which resulted in serious errors. In the case of Pietrzyk et al. [21], they used highly toxic UV-C light, which that made progenitor cells mortal regardless of the labeling, and thus, made a real dormant fraction missing. In the case of Hagan and colleagues [22,23], they used UV-B light, and found plateau phases of a surviving colony fraction with increasing dose of UV-B fluence (J/m^2) after increasing the period of BrdUrd infusion. The fraction containing cycling one measured on the basis of colony formation still exponentially increases >90%. Use of UV-A and incorporation of BrdUrd in drinking water for long-term administration collaboratively provided a revolutionary paradigm for increasing the knowledge of kinetics in the hemopoietic stem/progenitor cell compartment.

A new discovery is the existence of a long-term and stable, dormant fraction. This is similar to crypt stem cells at the bottom of intestinal villi, described by Potten et al. [24], but never clearly observed in the hemopoietic system. The dormant fraction develops presumably after the early developmental stage of the neonatal period, which forms an orderly generation-age structure from a primitive CFU-S-13, mature CFU-S-9, and to an in vitro CFU-GM (21.7% ± 4.7%, 33.4% ± 3.3%, and 35.0% ± 3.7%, respectively [11]). Second, by BUUV assay, some disadvantages of in vitro labeling with ^{3}H-TdR and also with BrdUrd were consequently discovered; e.g., in vitro labeling artificially results in a marked overestimation of the percentage of the labeled fraction from 9.9% ± 4.8% to 37.4% ± 4.5%. The cycling fraction of CFU-GM is often labeled and assayed in vitro. The in vivo labeling assay value is

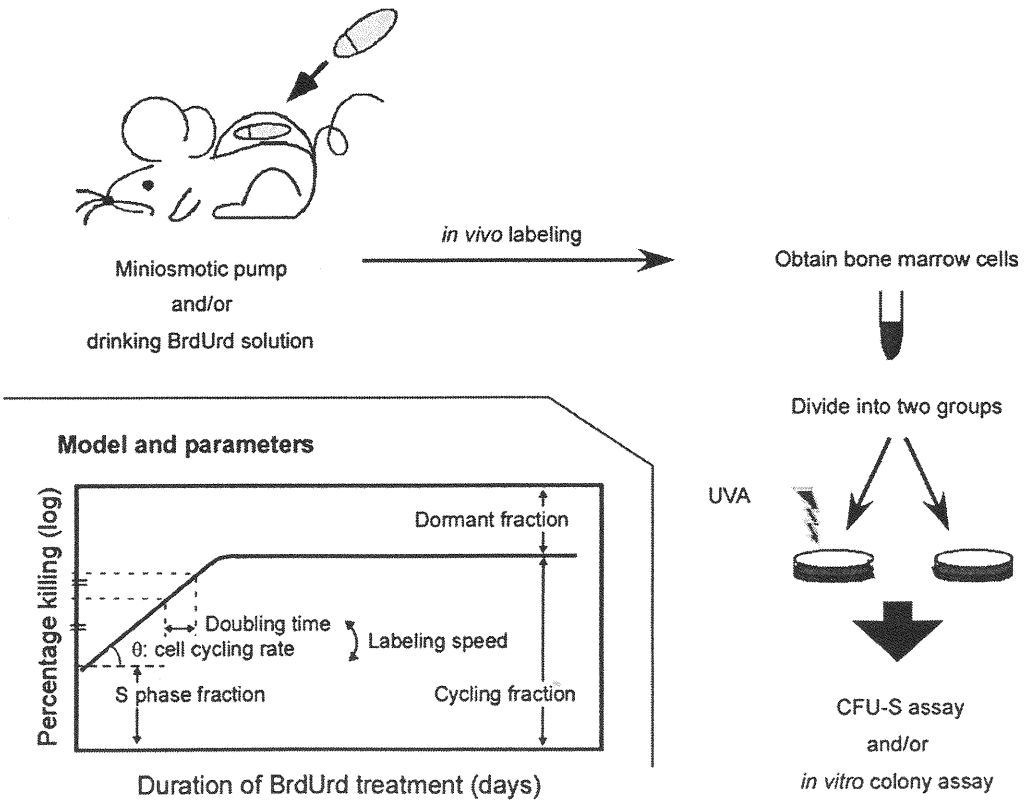

Figure 2. Bromodeoxyuridine UV method as a tool for evaluating size and other parameters of cycling stem cell fraction in vivo [12].

only slightly higher than the actual CFU-S cycling fraction when assayed by in vivo labeling, regardless of the labeling method; that is, intravenous injection or via drinking water (9.9% ± 4.8% vs 6.8% ± 4.8%; CFU-GM vs CFU-S-9, respectively). Many previous studies showed that CFU-GM and other in vitro colonies labeled with ^{3}H-TdR cytocide were nearly 60% in cycling, which was used as an indicator of the maturity of progenitor cells in vitro in terms of generation age, but are now considered artifacts.

The doubling time and the generation time of each progenitor cell compartment are also dependent on the age-structure, and the doubling times are from 35.2 hours in CFU-S-13, 48.5 hours in CFU-S-9 to 56.0 hours in CFU-GM, respectively [11]. For example, in the cases of caloric restriction and 3′-azido-3′-deoxythymidine treatment, both markedly decreased the cycling fraction of the hemopoietic stem/progenitor cell compartment [8,9,25].

Radiation-induced leukemogenesis and its prevention by caloric restriction

As shown in Figure 1A, the incidence of radiation-induced leukemias depends on two functions: one is stem/progenitor cell survival with graded increases in radiation dose and the other is the minimum number of potentially mutated stem/progenitor cells for the development of one case of leukemia vs graded increases in doses of radiation. Because the integral of the shaded channel area in Figure 1 decreases with the increase in radiation doses and the channel is closed at 6 to 7 Gy, radiation-induced leukemias are not supposed to develop at more than 6 to 7 Gy in the murine system. In the case of p53-deficient mice, however, despite radiation-induced damage, the survival of hemopoietic progenitor cells with the increase in radiation dose shows a much shallower survival curve (Fig. 1B, line "a"), owing to their escape from p53-dependent apoptosis; these cells may retain unrepairable DNA damage (data not shown; [13,26]). This modification of the survival curve of hemopoietic stem/progenitor cells deficient in p53 further increases the incidence of radiation-induced leukemias, and the incidence of leukemias following 5-Gy exposure keeps increasing up to 100% (unpublished data).

Next, we modified radiation-induced leukemogenesis by caloric restriction, because caloric restriction is the only nutritional factor that extends lifespan of experimental animals [27], and is supposed to attenuate radiation-induced leukemias [9]. The C3H/He mouse strain shows a high incidence of myeloid leukemias, with a low spontaneous incidence (of myeloid leukemia). Nonirradiated mice showed a 1% incidence of spontaneous myeloid leukemias with a median lifetime of 839 days. The incidence of myeloid leukemias increased up to 22.2% with a decrease in median lifetime to 697 days after the 3-Gy whole-body x-ray irradiation of mice. Various methods of caloric restriction induced a prominent decrease in the incidence of myeloid leukemias at 3 Gy; i.e., 9.5% in the group with caloric restriction for the rest of their lifetime immediately after the irradiation; 8.0% in the group with caloric restriction throughout their lifetime. No leukemia developed in groups not exposed to radiation (data not shown; [9]).

Along with the decrease in the incidence of myeloid leukemia in the group with caloric restriction, interestingly, the percentages of tumor-free mice consequently increased from 7.4% to 17.5% and 20.0%, in the group with caloric restriction for the rest of their lifetime after 3-Gy irradiation and in the group with caloric restriction throughout their lifetime, respectively. Nonirradiated group with caloric restriction also showed a statistically significant increase 10.1% to 46.4% in the percentage of tumor-free mice as compared with groups without caloric restriction.

Because caloric restriction decreased the number of hemopoietic stem/progenitor cells and the cycling fraction of hemopoietic progenitor cells, as evaluated by the BUUV method in these series of experiments, we conclude that caloric restriction decreases the incidence of radiation-induced leukemias via two mechanisms. First, the suppression of direct genotoxic leukemogenesis during the initiation stage, i.e., caloric restriction started before irradiation and continued until irradiation. Second, the suppression of indirect epigenetic leukemogenesis during the promotor stage, i.e., restriction started after irradiation and continued for lifetime. In these studies of caloric restriction, particular attention was focused on the number and cell cycle of hemopoietic stem/progenitor cells regardless of other suppressive factors that may also contribute to general oncogenesis, such as oncogene expression, DNA methylation, free radical formation, apoptosis induction and immunity activation, among others.

Benzene-induced hemopoietic toxicities and induction of leukemias, and their attenuation by thioredoxin overexpression

Cronkite was the first scientist who clearly recognized the relevance of the number and position of hemopoietic stem/progenitor cells in their kinetics with respect to the development of leukemias [28]. Consequently, his benzene exposure protocol successfully induced the first experimental benzene-induced leukemias; namely, the induction of a modest decrease in the number of hemopoietic progenitor cells that does not lead to extinction of such cells [2], which was after the first report of leukemogenicity induced in humans nearly 80 years ago [29]. He was interested in, and focused on, peculiar oscillatory changes in the numbers of bone marrow cells and hemopoietic progenitor cells, although laborious ^{3}H-TdR labeling for the complicated cell-cycle perturbation induced by benzene exposure could not help his group clarify the mechanism underlying cell-cycle oscillation. As reported by our group previously in *Experimental Hematology* [7], benzene exposure was found to be not only in mature blood cells, but also in hemopoietic stem/progenitor cells, a strong cell-cycle suppressor, due to clastogenic

damages suggested by an upregulation of topoisomerase III in the bone marrow [30]; however, cessation of benzene exposure during weekends induced rapid recovery of the cycling of the hemopoietic stem/progenitor cell fraction, which induced the repeated counter-oscillatory changes during the exposure period and resulted in a high frequency of epigenetic induction of hemopoietic malignancies (Fig. 3). Benzene and its major metabolites are negative in Ames-revertant mutagenesis assay, and induce a lesser amount of DNA adducts, which cannot explain in detail the mechanism underlying leukemogenicity. Benzene-induced cell-cycle perturbation observed in the present study may collaboratively cause clastogenic chromosomal damage induced by benzene mono-oxide and oxidative stress [30,31].

Conclusion from the base of bioinformatics: Experimental leukemogenesis and its attenuation with respect to related changes in Gompertzean survival curve

In the theoretical model of the mortality rate of human beings, studied by Gompertz [1] more than 180 years ago, he found that death rate during a unit time interval increases exponentially with lifetime. The Gompertzean expression can be applied to major mammalian species (Fig. 4A) [32]. The implication of Gompertzean linearity in experimental groups and changes in the slope linearity are considered to be based on an observation that lifespan may involve a function based on the multiplication of various life-threatening factors. Namely, the linearity is based on a system in which each lifespan-linked disease is independent and links to other diseases multiply (Eq. 1).

$$N'(t) = -rN(t)log(N(t)/K) \quad (1)$$

where $N(t)$ is number of individuals at time t, r is intrinsic growth rate, and K is number of individuals in equilibrium.

Furthermore, any continuous life-threatening factors except deaths from traffic accident, war, or epidemic infections, make Gompertzean linearity steeper (Fig. 4B: standard, "Std", to "Tox"). For example, in the case of mice exposed to graded increases in radiation dose, their lifespan shows continuously steeper curves from high-dose to zero-dose group, i.e., a steeper curve to a shallower

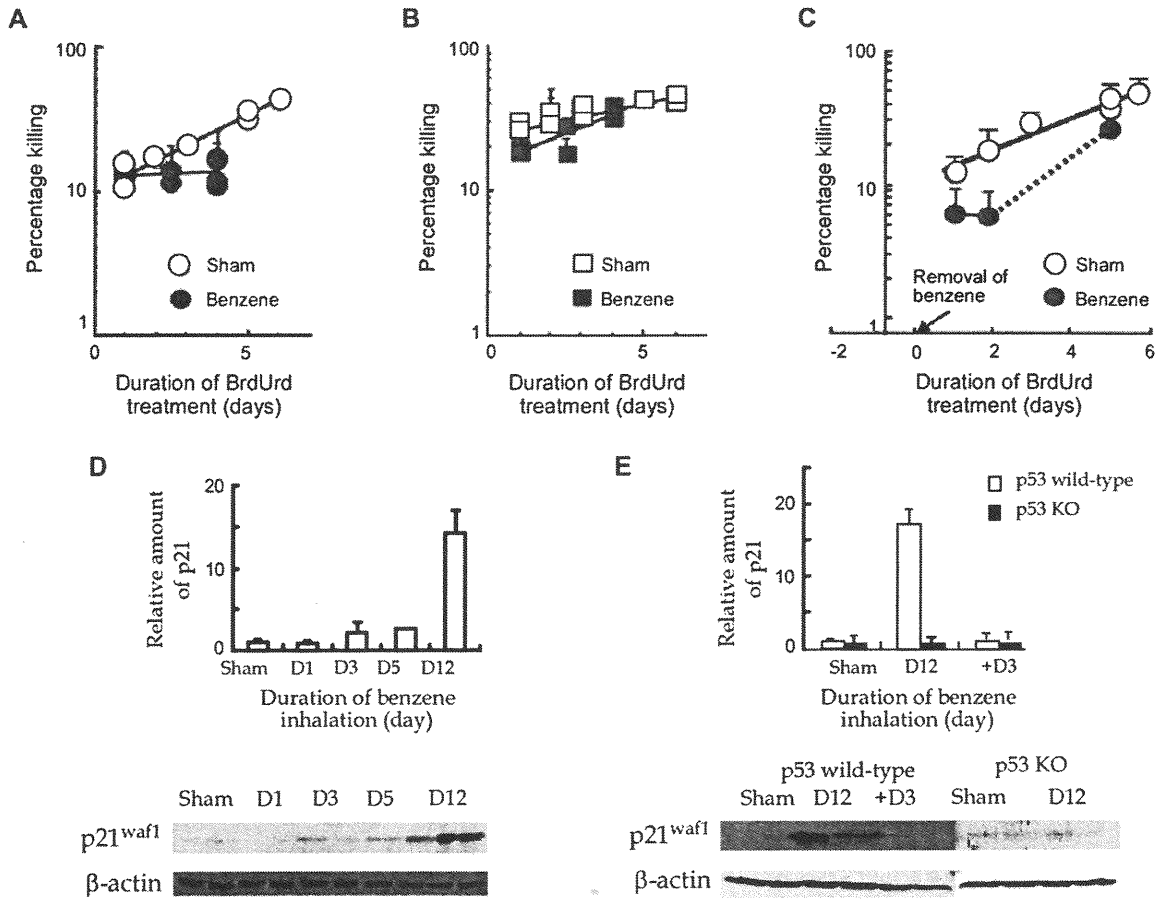

Figure 3. Benzene-induced cell-cycle arrest via p53-p21^{waf1} signal pathway [7]. (**A**) In wild-type mice, cell kinetics is stopping during the benzene inhalation (closed circles) vs sham control (open circles). (**B**) In p53-homozygous knockout mice, cell kinetics is maintained during benzene inhalation (closed squares) vs sham control (open squares). (**C**) After stopping benzene exposure, cell kinetics rapidly recovers in wild-type mice. (**D**) In wild-type mice, p21^{waf1} is upregulated during benzene inhalation. (**E**) In p53-homozygous knockout mice, p21^{waf1} is not changed during benzene inhalation. After stopping benzene inhalation, in wild-type mice, p21^{waf1} is downregulated immediately.

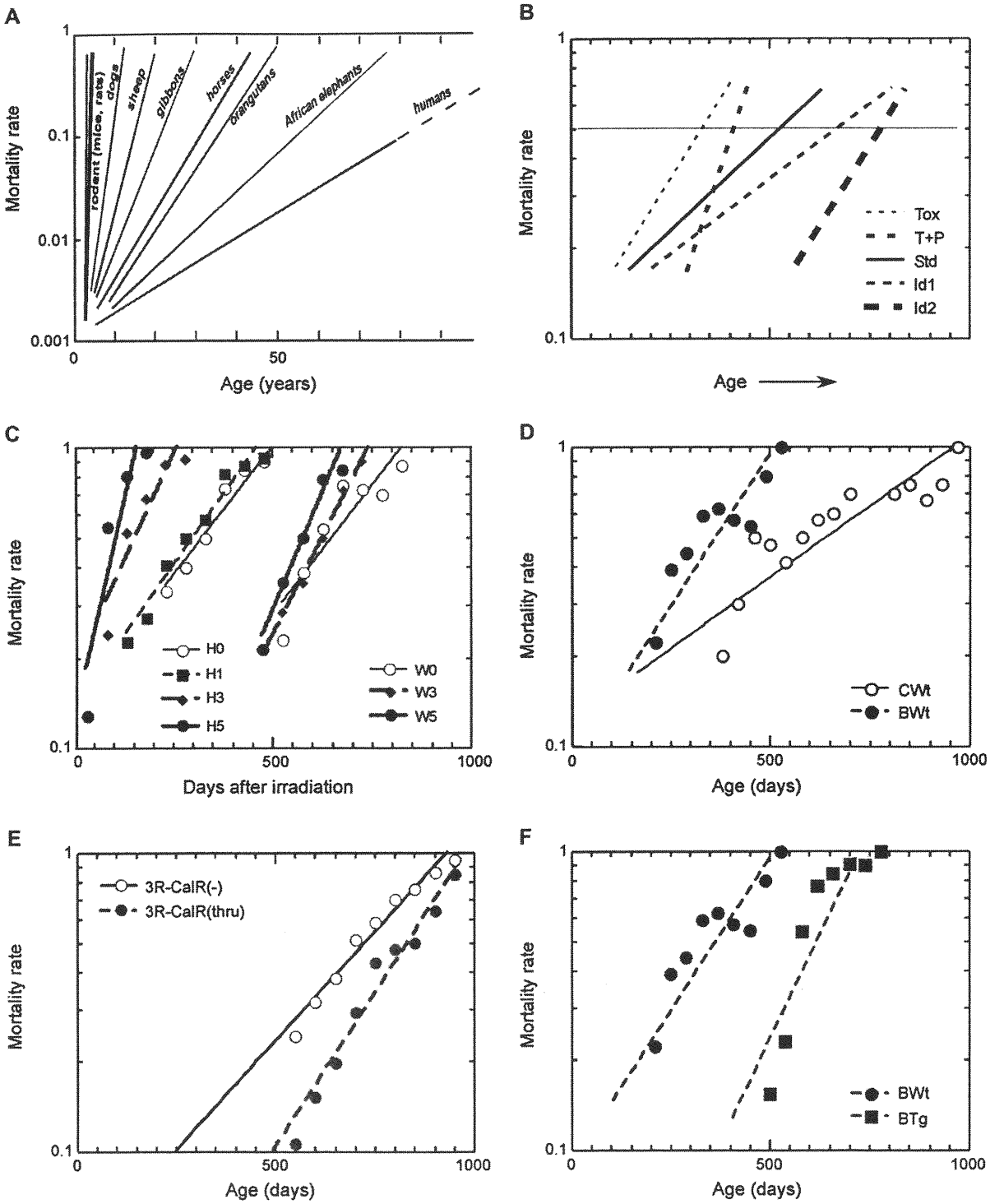

Figure 4. Gompertz's low of mortality was applied to examine lifespans and mortality rates in mice with ionizing radiation (IR)- and benzene-induced leukemias. (**A**) Lifespan in the steady-state animals, based on the life expectancy. (**B**) Gompertz model for lifespan in toxic changes and its attenuations. Tox = toxic state; T+P = toxic state with prevention; Std = standard; Id = ideal state). (**C**,**E**) Radiation-induced shortening of lifespan. (**C**) H0 to H5 = p53-heterozygous knockout mice with 0 to 5 Gy whole-body irradiation; W0 to W5 = wild-type mice with 0 to 5 Gy whole-body irradiation and its recovery by caloric restriction. (**E**) 3R-CalR(−); 3-Gy irradiation without caloric restriction, 3R-CalR(thru); 3-Gy irradiation with caloric restriction). Average caloric intake calculated was 77 kcal per week per mouse (i.e., 81.1% of the nonrestrict control). Detailed technical information for caloric restriction can be found elsewhere [9]. (**D**,**F**) Benzene-induced shortening of lifespan. (**D**) CWt = wild-type mice for sham control; BWt = wild-type mice with benzene exposure) and recovery by Trx overexpression. (**F**) BWt = wild-type mice with benzene exposure; BTg = thioredoxin overexpression mice with benzene exposure. Benzene was exposed at 300 ppm, 6 hours per day, 5 days a week, for 26 weeks. For Trx overexpression mice, detailed technical information can be found elsewhere [5,31].

curve (Fig. 4C). In Figure 4C, H0 through H5 indicate p53 heterozygous-deficient mice exposed to graded increases in dose of radiation (0–5 Gy), which show more steeper and shortened lifespans. Similarly, benzene-induced leukemias make the lifespan curve in the Gompertzean expression also steeper with benzene exposure (Fig. 4D). Although these slopes seem to be based on the incidence of various types of tumorigenesis, the slopes may be modified by other chronic factors, such as nutrition related to cardio- and/or renal-vascular diseases. Two prevention studies provide interesting prevention curves in Gompertzean expression; one on caloric restriction in radiation-induced leukemogenesis [9] and the other on thioredoxin overexpression against benzene toxicity [31], which shows potentially equivalent antioxidative functions (Fig. 4E and F). Gompertzean expression curves for toxic compounds and for inhibitory compounds shown in Figure 4C to F imply that the slopes for Gompertzean expression may be based on the model shown in Figure 4B (Fig. 4E corresponds to "T+P (Tox & Prevention)" in Fig. 4B; Fig. 4F corresponds to ideal prevention, "Id 2" in Fig. 4B.). The significance of differences in slopes in Gompertzean expression among the non-treated animals, animals treated with toxic compounds, and animals treated with inhibitory compounds, and possible deterministic factors for genomic stabilization, cell-cycle regulators and active caloric metabolic enzymes, among others, are not clearly understood. However, this relevance would be an important factor for elucidating the mechanism underlying toxicities vs prevention of lifespan.

Acknowledgments

The authors would like to thank the collaborators for valuable assistance. This work was supported in part by the fund from Nuclear Research of MEXT, Japan, the Human Sciences of Japan (KH31034, KHC1204), Grants-in-Aid (Nos.13670236, 15510064, 16590329 and 18510066) for Scientific Research C from the Japan Society for the Promotion of Sciences, and Risk Analysis Research on Food and Pharmaceuticals for Health and Labor Science Research Grants (H15-Chemicals-002, H16-Chemicals-002).

References

1. Gompertz B. On the nature of the function expressive of the law of human mortality, and on a new mode of determining the value of life contingencies. Pholos Trans Royal Soc (Lond). 1825;115:513–585.
2. Cronkite EP, Inoue T, Carsten AL, Miller ME, Bullis JE, Drew RT. Effects of benzene inhalation on murine pluripotent stem cells. J Toxicol Environ Health. 1982;9:411–421.
3. Cronkite EP. Hemopoietic stem cells: an analytic review of hemopoiesis. Pathobiol Annu. 1975;5:35–69.
4. Tsukada T, Tomooka Y, Takai S, et al. Enhanced proliferative potential in culture of cells from p53-deficient mice. Oncogene. 1993;8:3313–3322.
5. Mitsui A, Hirakawa T, Yodoi J. Reactive oxygen-reducing and protein-refolding activities of adult T cell leukemia-derived factor/human thioredoxin. Biochem Biophys Res Commun. 1992;186:1220–1226.
6. Cronkite EP, Bullis J, Inoue T, Drew RT. Benzene inhalation produces leukemia in mice. Toxicol Appl Pharmacol. 1984;75:358–361.
7. Yoon BI, Hirabayashi Y, Kawasaki Y, et al. Mechanism of action of benzene toxicity: cell cycle suppression in hemopoietic progenitor cells (CFU-GM). Exp Hematol. 2001;29:278–285.
8. Yoshida K, Inoue T, Hirabayashi Y, Matsumura T, Nemoto K, Sado T. Radiation-induced myeloid leukemia in mice under calorie restriction. Leukemia. 1997;11(suppl 3):410–412.
9. Yoshida K, Hirabayashi Y, Watanabe F, Sado T, Inoue T. Caloric restriction prevents radiation-induced myeloid leukemia in C3H/HeMs mice and inversely increases incidence of tumor-free death: implications in changes in number of hemopoietic progenitor cells. Exp Hematol. 2006;34:274–283.
10. Till JE, McCulloch EA. A direct measurement of the radiation sensitivity of normal mouse bone marrow cells. Radiat Res. 1961;14:213–222.
11. Hirabayashi Y, Matsuda M, Aizawa S, Kodama Y, Kanno J, Inoue T. Serial transplantation of p53-deficient hemopoietic progenitor cells to assess their infinite growth potential. Exp Biol Med (Maywood). 2002;227:474–479.
12. Hirabayashi Y, Matsumura T, Matsuda M, et al. Cell kinetics of hemopoietic colony-forming units in spleen (CFU-S) in young and old mice. Mech Ageing Dev. 1998;101:221–231.
13. Yoshida K, Aizawa S, Watanabe K, Hirabayashi Y, Inoue T. Stem-cell leukemia: p53 deficiency mediated suppression of leukemic differentiation in C3H/He myeloid leukemia. Leuk Res. 2002;26:1085–1092.
14. Milner LA, Kopan R, Martin DI, Bernstein ID. A human homologue of the Drosophila developmental gene, Notch, is expressed in CD34+ hematopoietic precursors. Blood. 1994;83:2057–2062.
15. Reya T, Duncan AW, Ailles L, et al. A role for Wnt signalling in self-renewal of haematopoietic stem cells. Nature. 2003;423:409–414.
16. Bhardwaj G, Murdoch B, Wu D, et al. Sonic hedgehog induces the proliferation of primitive human hematopoietic cells via BMP regulation. Nat Immunol. 2001;2:172–180.
17. Lessard J, Sauvageau G. Bmi-1 determines the proliferative capacity of normal and leukaemic stem cells. Nature. 2003;423:255–260.
18. Sasaki H, Matsuda M, Lu Y, et al. A fraction unresponsive to growth inhibition by TGF-beta among the high-proliferative potential progenitor cells in bone marrow of p53-deficient mice. Leukemia. 1997;11:239–244.
19. Cronkite EP. Kinetics of leukemic cell proliferation. Semin Hematol. 1967;4:415–421.
20. Cronkite EP. Regulation and structure of hemopoiesis: Its application in toxicology. In: Iron RD, ed. Toxicology of the Blood and Bone Marrow. New York: Raven Press; 1985. p. 17–38.
21. Pietrzyk ME, Priestley GV, Wolf NS. Normal cycling patterns of hematopoietic stem cell subpopulations: an assay using long-term in vivo BrdU infusion. Blood. 1985;66:1460–1462.
22. Hagan M, Patchen M, Weinberg S, MacVittie T. Erythroid progenitor (BFU-E, CFU-E) proliferation as inferred from 5′bromodeoxyuridine labeling. Exp Hematol. 1994;22:1221–1226.
23. Hagan MP, MacVittie TJ. CFUs kinetics observed in vivo by bromodeoxyuridine and near-UV light treatment. Exp Hematol. 1981;9:123–128.
24. Potten CS, Chadwick C, Ijiri K, Tsubouchi S, Hanson WR. The recruitability and cell-cycle state of intestinal stem cells. Int J Cell Cloning. 1984;2:126–140.
25. Inoue T, Cronkite EP, Hirabayashi Y, Bullis JE Jr, Mitsui H, Umemura T. Lifetime treatment of mice with azidothymidine (AZT) produces myelodysplasia. Leukemia. 1997;11(suppl 3):123–127.

26. Hirabayashi Y, Matsuda M, Matumura T, et al. The p53-deficient hemopoietic stem cells: their resistance to radiation-apoptosis, but lasted transiently. Leukemia. 1997;11(suppl 3):489–492.
27. MacCay CM, Crowell MF, Maynard MF. The effect of retarded growth upon the length of the lifespan and upon the ultimate body size. J Nutr. 1935;10:63–79.
28. Cronkite EP, Bullis J, Inoue T, Drew RT. Benzene inhalation produces leukemia in mice. Toxicol Appl Pharmacol. 1984;75:358–361.
29. Delore P, Borgomano C. Leucémie aiguë au cours de l'intoxication benzénique. Sur l'origine toxique de certaines leucémies aiguës et leurs relations avec less anémies graves. J de méd de Lyon. 1928;9:227–233.
30. Yoon BI, Li GX, Kitada K, et al. Mechanisms of benzene-induced hematotoxicity and leukemogenicity: cDNA microarray analyses using mouse bone marrow tissue. Environ Health Perspect. 2003;111: 1411–1420.
31. Li GX, Hirabayashi Y, Yoon BI, et al. Thioredoxin overexpression in mice, model of attenuation of oxidative stress, prevents benzene-induced hemato-lymphoid toxicity and thymic lymphoma. Exp Hematol. 2006;34:1687–1697.
32. Trosko JE, Inoue T. Oxidative stress, signal transduction, and intercellular communication in radiation carcinogenesis. Stem Cells. 1997; 15(suppl 2):59–67.

J Membrane Biol (2007) 217:105–113
DOI 10.1007/s00232-007-9042-z

Membrane Channel Connexin 32 Maintains $Lin^-/c\text{-}kit^+$ Hematopoietic Progenitor Cell Compartment: Analysis of the Cell Cycle

Yoko Hirabayashi · Byung-Il Yoon · Isao Tsuboi · Yan Huo · Yukio Kodama · Jun Kanno · Thomas Ott · James E. Trosko · Tohru Inoue

Received: 30 April 2007 / Accepted: 14 May 2007 / Published online: 15 July 2007

Abstract Membrane channel connexin (Cx) forms gap junctions that are implicated in the homeostatic regulation of multicellular systems; thus, hematopoietic cells were assumed not to express Cxs. However, hematopoietic progenitors organize a multicellular system during the primitive stage; thus, the aim of the present study was to determine whether Cx32, a member of the Cx family, may function during the primitive steady-state hematopoiesis in the bone marrow (BM). First, the numbers of mononuclear cells in the peripheral blood and various hematopoietic progenitor compartments in the BM decreased in Cx32-knockout (KO) mice. Second, on the contrary, the number of primitive hematopoietic progenitor cells, specifically the $Lin^-/c\text{-}kit^+/Scal^+$ fraction, the KSL progenitor cell compartment, also increased in Cx32-KO mice. Third, expression of Cx32 was detected in $Lin^-/c\text{-}kit^+$ hematopoietic progenitor cells of wild-type mice (0.27% in the BM), whereas it was not detected in unfractionated wild-type BM cells. Furthermore, cell-cycle analysis of the fractionated KSL compartment from Cx32-KO BM showed a higher ratio in the G_2/M fraction. Taken together, all these results imply that Cx32 is expressed solely in the primitive stem cell compartment, which maintains the stemness of the cells, i.e., being quiescent and noncycling; and once Cx32 is knocked out, these progenitor cells are expected to enter the cell cycle, followed by proliferation and differentiation for maintaining the number of peripheral blood cells.

Keywords Connexin 32 · Hematopoiesis · Hematopoietic stem cell · Cx32-knockout mouse

Y. Hirabayashi (✉) · B.-I. Yoon · I. Tsuboi · Y. Huo · Y. Kodama · J. Kanno
Division of Cellular and Molecular Toxicology, Center for Biological Safety and Research, National Institute of Health Sciences, 1-18-1 Kamiyohga, SetagayakuTokyo 158-8501, Japan
e-mail: yokohira@nihs.go.jp

B.-I. Yoon
Laboratory of Histology and Molecular Pathogenesis, School of Veterinary Medicine, Kangwon National University, Chuncheon 200-701, Republic of Korea

T. Ott
Service Einrichtung Transgene Tiere, Hertie-Institut für Klinische Hirnforschung, Tübingen 72076, Germany

J. E. Trosko
Department of Pediatrics and Human Development, Michigan State University, College of Human Medicine, East Lansing, MI 48824, USA

T. Inoue
Center for Biological Safety and Research, National Institute of Health Sciences, Tokyo 158-8501, Japan

Introduction

Connexin (Cx) functions in the organization of cell-cell communication via gap junctions in multicellular organisms. Gap junctions have been implicated in the homeostatic regulation of various cellular functions, including growth control and differentiation (Loewenstein, 1979), apoptosis (Wilson, Close & Trosko, 2000) and the synchronization of electrotonic and metabolic functions (Bruzzone, White & Paul, 1996).

The role of Cxs in hematopoietic organs is poorly understood, except that the expression of Cx43 between hematopoietic progenitor cells and bone marrow (BM) stromal cells sustains hematopoiesis (Rosendaal, Gregan & Green, 1991; Ploemacher et al., 2000; Cancelas et al.,

2000; Montecino-Rodriguez, Leathers & Dorshkind, 2000). As Cxs are essential molecules for multicellular organisms, Cxs that organize cell-cell communication within the hematopoietic progenitor cell compartment are surmised to be present in BM tissue. If Cxs are present among hematopoietic progenitor cells, what would be their functions?

Krenacs & Rosendaal (1998) previously reported that Cx32 is not expressed in the BM. Therefore, if Cx32 is expressed in the blood cells, such Cx32-expressing cells would likely be, e.g., solely hematopoietic stem/progenitor cells. Such a specific study was supposed to be supported by the use of knockout (KO) mice for specific Cx molecules. Consequently, we found a functional impairment of the BM in Cx32-KO mice in our benzene exposure experiment (Yoon et al., 2004).

Cx32-KO mice were first established in 1996 by Willecke (Nelles et al., 1996). Using these Cx32-KO mice, an analysis of the possible functions of Cx32 in hematopoietic stem/progenitor cells was conducted using a reverse biological approach. Cx32-KO mice showed decreased numbers of peripheral mononuclear cells, various progenitor cell compartments and an increased primitive stem cell fraction, such as the lineage marker-negative (Lin^-)/c-kit-positive ($c\text{-}kit^+$)/stem cell antigen-1-positive ($Sca1^+$) (=KSL) fraction. On the contrary, in wild-type mice, expression of Cx32 was detected by immunocytochemistry and reverse transcriptase-polymerase chain reaction (RT-PCR), although it was not detected in unfractionated wild-type BM cells. Subsequent cell-cycle analyses, one for colony-forming progenitors using the method for evaluation of cycling progenitor cells with incorporation of bromodeoxyuridine (BrdUrd) followed by exposure to ultraviolet A (UVA) (see, BUUV Assay in Materials and Methods) and the other using a cell sorter with Hoechst 33342 for the KSL fraction, showed a significant increase in the ratio of the cell-cycle fraction in both compartments in the BM of Cx32-KO mice. The functions of Cx32, which is expressed in primitive hematopoietic stem/progenitor cells, are likely restoration of stem/progenitor cell quiescence and maintenance of primitive stem cells to prevent exhaustion.

Materials and Methods

Experimental Animals

Cx32-KO mice ($Cx32^{-/-}$ or $Cx32^{-/Y}$) were genetically modified from the F_1 embryonic cell line 129/J and the C57BL/6 strain developed by Willecke (Nelles et al., 1996). Heterozygous mice ($Cx32^{-/+}$) backcrossed with the C57BL/6 strain and maintained at the animal facility of the National Institute of Health Sciences (NIHS), Tokyo, Japan, were used. The pups were genotyped by PCR for screening of DNA from their tails.

Eight-week-old C57BL/6 male mice from Japan SLC (Hamamatsu, Japan) were used for the colonization assay. All experimental protocols involving laboratory mice in this study were reviewed by a peer review panel, the Interdisciplinary Monitoring Committee for the Right Use and Welfare of Experimental Animals, established at the NIHS, and approved by the Committee for Animal Care and Use at the NIHS with the experimental code 224-37009639415-2002.

Blood and BM Separation

The numbers of peripheral white blood cells, platelets and red blood cells were measured using a Coulter counter (Sysmex K-4500; Sysmex, Kobe, Japan). BM cells were harvested from the femur of each mouse (Yoon et al., 2001) after the animals were killed by cervical dislocation under deep anesthesia with ethyl ether. A 26-gauge needle was inserted into the femoral bone cavity through the proximal and distal ends of the bone shafts, and BM cells were flushed out under pressure by injecting 2 ml of α-minimum essential medium (α-MEM) with ribonucleosides and deoxyribonucleosides (Invitrogen, Carlsbad, CA).

Antibodies and Immunomagnetic Bead Separation

For the depletion of differentiated (lineage marker-positive) cells from BM cells, immunomagnetic bead separation (BD IMag Mouse Hematopoietic Progenitor Cell Enrichment™ set; BD Biosciences, San Jose, CA) or immunobead density gradient separation (SpinSep™; StemCell Technologies, Vancouver, Canada) was performed. As for lineage (Lin) markers, a biotinylated antibody cocktail (BD Biosciences) containing anti-mouse CD3e (145-2C11), CD11b (M1/70), CD45R/B220 (RA3-6B2), Ly-6G and Ly-6C/Gr-1 (RB6-8C5) and TER-119/erythroid cell (TER-119) antibodies and a monoclonal antibody cocktail (SpinSep) containing anti-CD5/Ly-1, CD45R, CD11b/Mac-1, Ly-6G/Gr-1, TER119 and 7/4/neutrophil antibodies were used. As a secondary antibody for the former biotinylated antibody cocktail, streptavidin (StAv)-coated beads (BD Biosciences) for depletion and StAv-peridinin chlorophyll-a protein (PerCP, BD Biosciences) for visualization were used. For the latter cocktail (SpinSep), an optimized combination antibody cocktail against it that had been coated on dense microparticles, i.e., SpinSep Mouse Dense Particles (StemCell Technologies), was used for immunoprecipitation.

For enrichment of the $c\text{-}kit^+$ fraction by immunomagnetic bead separation, CD117/c-kit-conjugated phycoerythrin (PE, StemCell Technologies) was used as a progenitor

marker and, as a secondary antibody, an anti-PE tetrameric antibody complex (StemCell Technologies) was used.

For detection of Cx32-positive cells by flow cytometry, a mouse anti-Cx32 monoclonal antibody from two sources (Chemicon International, Temecula, CA; Santa Cruz Technology, Santa Cruz, CA) as a primary antibody and an anti-mouse immunoglobulin (Ig) conjugated with fluorescein isothiocyanate (FITC) as a secondary antibody (BD Biosciences) were used.

For cell-cycle analysis by flow cytometry, as lineage markers, the same antibody cocktails from BD Biosciences were used. In addition, CD117/c-kit conjugated with allophycocyanin (APC), stem cell antigen (Sca1) antibody conjugated with PE and an AT-rich DNA-binding dye, Hoechst 33342 (Sigma, St. Louis, MO), were used.

Immunohistochemical Analysis

The same anti-Cx32 antibody (Chemicon International) was used as the primary antibody. As for the secondary antibody, a biotinylated horse anti-mouse Ig G (Vector Laboratories, Burlingame, CA) was used, and streptavidin labeled with peroxidase and 3,3′-diaminobenzidine was used to detect immunoreactivity (Vector Laboratories).

Enrichment of BM Cells in $Lin^-/c\text{-}kit^+$ Fraction

The $Lin^-/c\text{-}kit^+$ fraction is rich in hematopoietic stem cells (HSCs). To obtain a large number of $Lin^-/c\text{-}kit^+$ progenitor cell-enriched fraction in BM cells, a combination of immunobead density gradient and immunomagnetic bead separation techniques was carried out. First, for the depletion of lineage-positive BM cells, harvested BM cells were processed through an immunobead density gradient using a density-matched medium and dense microparticles coated with a cocktail of an optimized combination of antibodies called SpinSep (StemCell Technologies). Second, for the selection of the $c\text{-}kit^+$ fraction, immunomagnetic bead separation using magnetic nanoparticles with a magnetic holder was carried out according to the manufacturer's instruction (StemCell Technologies). For each procedure, the antibodies used are described under Antibodies and Immunomagnetic Bead Separation, above.

Flow-Cytometric Analysis using Anti-Cx32 Antibody

BM cells with or without fractionation for $Lin^-/c\text{-}kit^+$ HSC enrichment were stained with the biotinylated antibody cocktail of StAv-PerCP, c-kit-PE, the anti-Cx32 antibody and anti-mouse IgG conjugated with FITC. Flow-cytometric analysis was carried out using FACSVantage and FACSAria (both from BD Biosciences).

Flow-Cytometric Analysis for Cell Cycle of KSL Fraction

Lineage-depleted BM cells were stained with the biotinylated antibody cocktail with StAv-PerCP, c-kit-APC, Sca1-PE and Hoechst 33342. Flow-cytometric analysis was carried out using FACSAria.

BUUV Assay

Hematopoietic progenitor cell-specific kinetic studies were evaluated by continuous labeling by an osmotic minipump (Alza, Palo Alto, CA) of BrdUrd for cycling cells, followed by UVA exposure and hematopoietic colonization assay (BUUV assay, details in Hirabayashi et al., 1998, 2002).

Irradiation

In the assay of hematopoietic progenitor cells, recipient mice were exposed to a lethal radiation dose of 915 cGy, at a dose rate of 124 cGy per minute, using a ^{137}Cs-gamma irradiator (Gammacell 40 Exactor; MDS Nordin, Ottawa, Canada) with a 0.5-mm aluminum-copper filter.

Assay for Colony-Forming Units in Spleen

The Till & McCulloch (1961) method was used to determine the number of hematopoietic spleen colonies, i.e., colony-forming units in spleen (CFU-S), formed by hematopoietic progenitor cells. Aliquots of a BM cell suspension were used for evaluating the numbers of CFU-S. Spleens were harvested 9 or 13 days after BM transplantation for determining the number of CFU-S-9 or CFU-S-13 and then fixed in Bouin's solution. Macroscopic spleen colonies were counted under an inverted microscope at ×5.6. It was previously shown, using the C57BL/6 strain, that all colonies visible on days 9 and 13 originate from transplanted BM cells under the condition that the recipient mice are exposed to a lethal radiation dose of 915 cGy (Hirabayashi et al., 2002).

Assay for Granulocyte-Macrophage Colony-Forming Units

Granulocyte-macrophage colony-forming units (CFU-GM) were assayed in semisolid methylcellulose culture (Yoon et al., 2001; Hirabayashi et al., 2002). Briefly, 8×10^4 BM cells suspended in 100 μl of α-MEM were added to 3.9 ml of culture medium containing 1% methylcellulose (Nakarai-Tesque, Kyoto, Japan), 30% fetal calf serum (HyClone Laboratories, Logan, UT), 1% bovine serum albumin (Sigma), 10^{-4} M mercaptoethanol (Sigma) and 10 ng/ml murine granulocyte-macrophage

colony-stimulating factor (GM-CSF; R&D Systems, Minneapolis, MN). One-milliliter aliquots containing 2×10^4 cells were placed in 35-mm tissue culture wells (Nalgen Nunc International, Rochester, NY) in triplicate and incubated for 6 days in a fully humidified incubator at 37°C with 5% CO_2 in air. Colonies were counted using an inverted microscope at ×40 (Olympus Optical, Tokyo, Japan).

PCR Analysis for Genotyping

To detect Cx32 wild-type and Cx32-KO alleles, PCR analysis was performed using genomic DNA from the tail of each mouse, and synthetic oligonucleotides were used as primers (Nelles et al., 1996). To detect the wild-type allele, a 5′ primer (ccataagtcaggtgtaaaggagc) and a 3′ primer (agataagctgcagggaccatagg) were used; to detect the Cx32-KO allele, a common 5′ primer and a *neo*-primer (atcatgcgaaacgatcctcatcc) were used.

Reverse Transcription and PCR Analysis of Cx32 Expression

Expression of the gene encoding Cx32 was analyzed by reverse transcription followed by PCR. The total RNA from BM cells and other tissues was isolated using a Qiagen RNAeasy kit (Qiagen, Valencia, CA).

Statistical Analysis

The data obtained were stored in a computer and processed for statistical analysis using Student's *t*-test to evaluate the significance of differences in blood cell count, BM cellularity and the numbers of progenitor cells, CFU-GM, CFU-S-9 and CFU-S-13 between the wild-type group and the KO group. Differences with $p < 0.05$ were considered significant.

Results

Expression of Cx32 in Bone Marrow

Table 1 shows various blood cell parameters for the wild-type and Cx32-KO mice, with body weight and spleen weight as references. Although the total numbers of BM cells and red blood cells did not significantly differ between the wild-type mice and the Cx32-KO mice, the numbers of white blood cells and platelets from the peripheral blood, CFU-S-13 (primitive hematopoietic progenitor cells), CFU-S-9 (differentiated progenitor cells) and CFU-GM (progenitor cells cultured *in vitro*) were all significantly lower in the Cx32-KO mice than in the wild-type mice. These results suggest that the Cx32-KO mice have a potential disadvantage in hematopoiesis. However, when we studied the expression of Cx32 in BM cells by RT-PCR, as shown in Figure 1, neither the expression of Cx32 in the spleen (*not shown*) nor that in the BM was detected except in the positive known control, the hepatic tissue. Thus, the negative expression of Cx32 in BM cells is in good agreement with a previous observation (Krenacs & Rosendaal, 1998).

Table 1 Parameters associated with steady-state hematopoiesis

Parameter	Wild-type	Cx32-KO
Body weight (g)	22.6 ± 1.97	22.5 ± 1.77
Spleen weight (mg)	77.8 ± 17.7	88.3 ± 9.6
BM cellularity ($\times 10^7$/femur)	2.28 ± 0.23	2.15 ± 0.08
Peripheral blood cells		
Red ($\times 10^7$/ml)	960 ± 30.8	930 ± 50.4
White ($\times 10^4$/ml)*	7,300 ± 283	5,633 ± 569
Platelets ($\times 10^7$/ml)*	67.6 ± 0.14	48.7 ± 0.93
Hematopoietic progenitor cells		
CFU-GM ($\times 10^2$/femur)*	387 ± 33.5	251 ± 27.4
CFU-S-9 ($\times 10^2$/femur)*	45.8 ± 4.78	32.7 ± 5.23
CFU-S-13 ($\times 10^2$/femur)*	27.7 ± 3.35	21.1 ± 2.85

Each value is expressed as average (n = 6 for each genotype) ± standard deviation except for the value of the hematopoietic progenitor cells. The numbers of hematopoietic progenitor cells in steady-state CFU-GM, day-9 spleen colonies (CFU-S-9) and day-13 spleen colonies (CFU-S-13) are expressed as average (three donor mice were used for each genotype, and six mice were used for each recipient group) ± standard deviation

* The difference calculated by *t*-test between wild-type and Cx32-KO is significant ($p < 0.05$)

We next studied Cx32 expression in colonies developed in the spleen in lethally irradiated wild-type recipient mice after injection of BM cells from wild-type mice or from Cx32-KO mice. Hematopoietic spleen colonies consist of a large number of immature cells rather than cells from the peripheral blood or unfractionated BM cells (Hirabayashi et al., 2002). Expression of Cx32 detected by RT-PCR analysis was only observed in the hematopoietic spleen colonies derived from wild-type BM cells (Fig. 1, lanes A1, A2). Expression of Cx32 was not detected in colonies derived from Cx32-KO BM cells, which are negative controls (Fig. 1, lanes B1, B2). Expression of Cx32 was also detected in spleen colonies from Cx32-KO recipient mice that had been repopulated with wild-type BM cells (Fig. 1, lanes C1, C2).

Immunohistochemical staining with the anti-Cx32 antibody was carried out to examine the hematopoietic spleen colonies originating from BM cells from wild-type mice and from Cx32-KO mice. A colony originating from a wild-type BM cell showed mild and mottled staining in the outer boundary of the spleen colonies, whereas a colony originating from Cx32-KO BM cells showed no staining

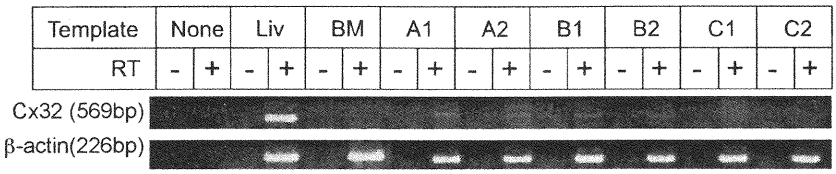

Fig. 1 Expression of Cx32 in BM and hematopoietic spleen colonies. Total RNAs were extracted for RT-PCR from the liver (*Liv*) and BM of wild-type mice and CFU-S-9. Note that Cx32 expression was not detected in the BM but was detected in the liver, which is a positive control (see Materials and Methods). To obtain CFU-S, lethally irradiated wild-type mice were injected with BM cells from wild-type or Cx32-KO donor mice. After 9 days, total RNAs extracted from individual hematopoietic spleen colonies derived from wild-type BM cells or those from Cx32-KO BM cells were reverse-transcribed, followed by PCR and then loaded (lanes *A1, A2, C1* and *C2*). Also, total RNAs extracted from the colonies derived from wild-type BM cells obtained from lethally irradiated Cx32-KO recipient mice followed by repopulation with wild-type BM cells were similarly loaded (lanes *B1* and *B2*). RT(+) and RT(-): with or without avian reverse transcriptase, 2.5 U/20 μl, respectively (see Materials and Methods)

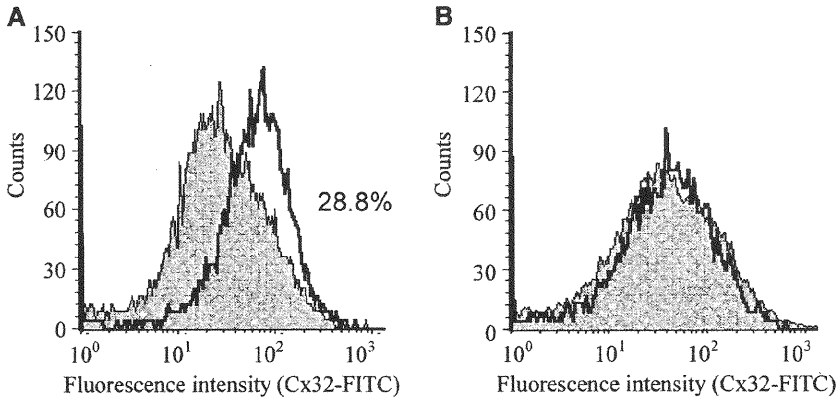

Fig. 2 Flow-cytometric analyses of $Lin^-/c\text{-}kit^+$ Cx32-positive cells from wild-type mice. Flow cytometry after BM cell separation was carried out by a combination of immunobead density gradient separation and immunomagnetic bead separation. Histogram of FITC-labeled anti-Cx32 antibody. $Lin^-/c\text{-}kit^+$ fraction (**a**) and $Lin^+/c\text{-}kit^-$ fraction (**b**) for wild-type BM cells (*open profile with bold line*) and same fractions for Cx32-KO BM cells (*shaded profile*), negative control. The Cx32-positive fraction shown in **a** calculated for the $Lin^-/c\text{-}kit^+$ fraction in wild-type BM cells is 28.8%

(*data not shown*). The findings described above suggest expression of Cx32 in the hematopoietic progenitor cells or stem cells alone; thus, further precise experiments were conducted.

Expression of Cx32 in $Lin^-/c\text{-}kit^+$ Hematopoietic Progenitor Cell Compartment

We determined whether Cx32-positive cells are consistently found in the HSC compartment. First, the $Lin^-/c\text{-}kit^+$ HSC-enriched fraction was obtained by the combination of immunobead density gradient separation for depleting lineage-positive cells and immunomagnetic bead separation for selecting $c\text{-}kit^+$ cells, followed by flow-cytometric analysis using the anti-Cx32 antibody. The separated $Lin^-/c\text{-}kit^+$ HSC fraction was 0.25% of the original unfractionated wild-type BM cells. The proportion of the $Lin^-/c\text{-}kit^+$ compartment (HSC compartment) is 90.2% of the $Lin^-/c\text{-}kit^+$ HSC-enriched preseparated fraction. Furthermore, the number of $Lin^-/c\text{-}kit^+$ compartments is 106.9-fold higher than the fraction of the original unfractionated BM cells. To determine which fraction Cx32-positive cells belong to, BM cells from wild-type mice and Cx32-KO mice with or without $Lin^-/c\text{-}kit^+$ HSC enrichment were stained with biotinylated antibody cocktail labeled with StAv-PerCP, c-kit-PE and Cx32-FITC. In wild-type BM cells, 28.8% of the $Lin^-/c\text{-}kit^+$ fraction was found to be Cx32-positive compared with the same fraction of BM cells obtained from Cx32-KO mice, which was used as the negative control (Fig. 2a). Together with the frequency data for the $Lin^-/c\text{-}kit^+$ HSC-enriched fraction, the fraction of Cx32-positive cells was calculated to be nearly 0.27% of the original unfractionated whole BM cells.

Whether the mature cell fraction, i.e., the $Lin^+/c\text{-}kit^-$ fraction, contains Cx32-positive cells, the fraction of the wild-type BM cells is compared with that of the control profile from the Cx32-KO mice. Because both fractions are nearly identical (Fig. 2b), few cells may be positive for Cx32 in the $Lin^+/c\text{-}kit^-$ fraction. The fraction of Cx32-positive cells is 0.0093% of the original unfractionated whole BM cells (*data not shown*).

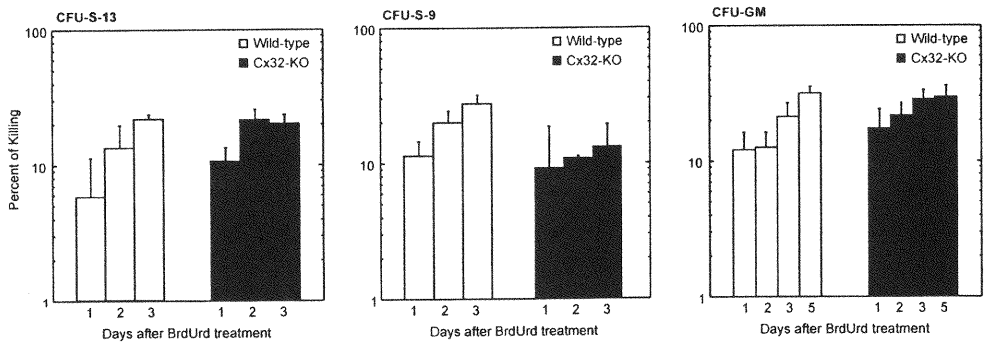

Fig. 3 The BrdUrd-labeled cells with an osmotic minipump purged by UVA light (BUUV) assay for evaluating the cycling fractions of the hematopoietic colonizing progenitor cells. Percent decreases in number of colonies compared with nonexposed control are shown along the ordinate axis (log.) vs. days for continuous labeling of BrdUrd with osmotic minipumps shown along the horizontal axis. CFU-S-13 (primitive hematopoietic progenitor cells), CFU-S-9 (differentiated progenitor cells) and CFU-GM (progenitor cells assayed by *in vitro* colonization) are shown. Each column represents 10 mice assayed for CFU-S-13 and six mice assayed for CFU-S-9

Function of Cx32 in Cell-Cycle Regulation in Hematopoietic Progenitor/Stem Cells

A significant decrease in the number of hematopoietic progenitor cells was observed in the Cx32-KO mice but without any significant difference in the decrease in BM cell number (Table 1), suggesting cell-cycle perturbation in the hematopoietic progenitor cells or stem cell compartment. Whether cell cycles are accelerated or decelerated in either the hematopoietic progenitor cell fractions or the hematopoietic stem cell compartment or both is not known. To characterize hematopoietic progenitor-specific cell cycle, the BUUV assay was conducted. To observe possible changes in the cell cycle in the hematopoietic stem cell compartment, the KSL fraction was assayed with Hoechst 33342 and possible changes in the ratio of G_0/G_1 were evaluated.

BUUV assay Hematopoietic stem cell-specific kinetics evaluation by continuous infusion of BrdUrd for cycling cells including hematopoietic progenitor cells followed by UVA exposure and hematopoietic progenitor colonization assay was conducted.

Results are shown in Figure 3. For CFU-S-13 (primitive hematopoietic progenitor cells), the incorporation of BrdUrd starts from a higher percentage with rapid increase in Cx32-KO mice, suggesting suppression of the cell cycle in these primitive hematopoietic progenitor cells with Cx32-mediated cell-cycle regulation in the wild-type steady state. This suppression may be attenuated in CFU-S-9, a differentiated progenitor cell compartment. For CFU-GM, the progenitor cells assayed by *in vitro* colonization also showed an accelerated cell cycle in Cx32-KO mice. The population doubling time calculated for each progenitor cell compartment is shown in Table 2.

Flow-cytometric analysis of KSL fraction Following the incorporation of the bioactive AT-rich DNA-binding dye Hoechst 33342, the lineage-depleted BM cells were analyzed by flow cytometry. The sizes of the $Lin^-/c\text{-}kit^+/Sca1^+$ (KSL) fraction obtained were 0.052% in the Cx32-KO BM cell compartment and 0.035% in wild-type BM cells (Table 3, Fig. 4a; $p = 0.0458 < 0.05$). The lineage-depleted BM cells were analyzed for their cell-cycle patterns by flow cytometry (Fig. 4b,c), and then G_0/G_1 was calculated for the $Lin^-/c\text{-}kit^+$ and KSL fractions for both the Cx32-KO and wild-type mice. The percentage of G_0/G_1 calculated for the $Lin^-/c\text{-}kit^+$ and KSL fractions were slightly lower in Cx32-KO mice (Table 4; 83.3% vs. 87.2% for Cx32-KO vs. wild-type for the $Lin^-/c\text{-}kit^+$ fraction, 89.2% vs. 91.5% for Cx32-KO vs. wild-type for

Table 2 Doubling times of hematopoietic progenitor cells

Progenitor cell	Genotype	Slope (%killing/day)[a]	*y* intercept (%)[a]	Population doubling[b] (h)	*r*
CFU-GM	Wild-type	0.255	9.09	28.3	0.973
	Cx32-KO	0.244	13.54	29.6	0.995
CFU-S9	Wild-type	0.440	7.62	16.4	0.986
	Cx32-KO	0.179	7.82	40.3	0.999
CFU-S13	Wild-type	0.659	3.16	11.0	0.988
	Cx32-KO	0.694	5.35	10.4	0.999

[a] Regression line: $y = b\ 10^{(ax)}$, where x is the duration after BrdUrd treatment (days), y is the percentage of killing, a is cell cycle velocity (coefficient) and b is the cycling ratio/unit time (coefficient)

[b] Doubling time (h) = (log2/a) × 24

Table 3 Incidence of hematopoietic stem cell fraction/femoral BM cells

Hematopoietic stem cell fraction	Wild-type	Cx32-KO	p^*
Lin^--c-kit^+ fraction (%)	0.316 ± 0.007	0.412 ± 0.022	0.0010
KSL fraction (%)	0.035 ± 0.008	0.052 ± 0.011	0.0458

Each value is expressed as average (n = 3 for each genotype) ± standard deviation

* The difference between wild-type and Cx32-KO was calculated by t-test

the KSL fraction; $p = 0.0126$ and $p = 0.0556$, respectively). The results suggest that Cx32 may have a suppressive function on such a hematopoietic stem cell compartment, KSL, under the physiological condition of Cx32.

Discussion

The role of Cx32 in steady-state hematopoiesis was analyzed in this study. This is the first observation of a Cx gene, namely *Cx32*, that is expressed in hematopoietic stem/progenitor cells. The functions of Cx32 in hematopoiesis were also investigated. In Cx32-KO mice, the numbers of various hematopoietic progenitor cells in the BM were lower than those in wild-type mice, suggesting a beneficial role of Cx32 for maintaining hematopoiesis during the steady state. Because the cell-cycle analyses of the hematopoietic stem cells, namely, the Lin^-/c-kit^+/$Sca1^+$ KSL, or the progenitor cells, Lin^-/c-kit^+ fractions, suggested a slightly but significantly higher incidence of a dormant stem cell fraction in wild-type mice, the physiological role of Cx32 is probably to maintain

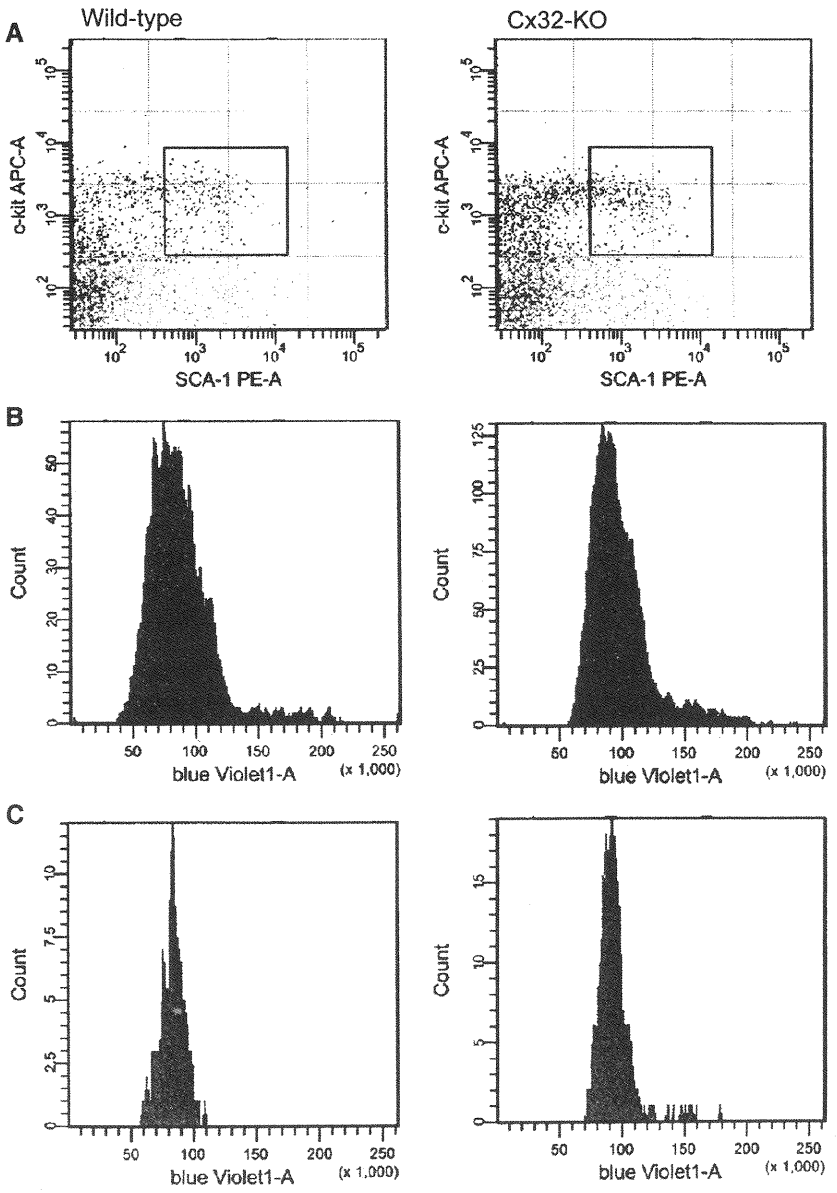

Fig. 4 **a** Two-dimensional expression shown by flow-cytometric analysis between c-kit and Sca1 expression on cells gated by lineage-negative fractions: wild-type and Cx32-KO mice. *Box* represents the c-kit^+/$Sca1^+$ fraction; thus, it is equivalent to the KSL fraction. **b**, **c** Flow-cytometric histograms showing reaction to Hoechst 33342 for Lin^-/c-kit^+ fraction (**b**) and Lin^-/c-kit^+/$Sca1^+$ (=KSL) fraction (**c**)

Table 4 G_0/G_1 ratio of hematopoietic stem cell fraction

Hematopoietic stem cell fraction	Wild-type	Cx32-KO	p*
$Lin^-/c\text{-}kit^+$ fraction (%)	87.2 ± 0.76	83.3 ± 1.75	0.0126
KSL fraction (%)	91.5± 2.53	89.2 ± 1.82	0.0556

Each value is expressed as average (n = 3 for each genotype) ± standard deviation

* The difference between wild-type and Cx32-KO was calculated by t-test

the quiescence of the primitive hematopoietic stem cell compartment, thereby maintaining the stemness of the cells in the fraction.

Various Cxs are expressed in the stromal cells of the fetal liver (i.e., Cxs 43, 45, 30.3, 31 and 31.1) and the BM (i.e., Cxs 43, 45 and 31) (Cancelas et al., 2000). However, the contribution of Cxs to hematopoiesis was determined only on the basis of the effect of Cxs via stromal cell dependence; consequently, no Cxs were previously found in hematopoietic stem cells or progenitor cells (Krenacs & Rosendaal, 1998). However, in our recent study, interestingly, Cx32-KO mice exposed to benzene showed hematopoietic impairment more than wild-type mice; furthermore, the site of this impairment was not identified in either hematopoietic progenitor cells or stromal cells (Yoon et al., 2004).

Thus, we first determined whether hematopoietic progenitor cells express Cx32 molecules. As reported elsewhere (Yoon et al., 2004; Nelles et al., 1996), no Cx32 was detected in unfractionated BM cells by either RT-PCR or cell sorter analysis with an immunofluorescence antibody against Cx32 in this study (Figs. 1, 2). However, interestingly, hematopoietic spleen colonies, derived from hematopoietic progenitor cells and consisting of relatively immature hematopoietic cells, were found to express Cx32. This observation was also consistent with the immunohistochemical reaction of cells in the colonies with the anti-Cx32 antibody, in which Cx32-positive cells were only found along the border of each colony (*data not shown*). Subsequent flow-cytometric analysis using the anti-Cx32 antibody after performing the combination of immunobead density gradient separation and immunomagnetic bead separation showed that the most Cx32-positive fraction belonged to the HSC-enriched fraction, i.e., the $Lin^-/c\text{-}kit^+$ fraction (28.8% of the fraction) (Fig. 2a). It was calculated as only 0.27% with respect to the unseparated BM cells. Because RT-PCR or Northern blotting possibly detects >1% of expressing cells, these findings are in good agreement with a previous report on the absence of Cx32 expression in unseparated BM tissue (Cancelas et al., 2000). A hematopoietic disadvantage in progenitor cells associated with Cx32 deficiency was further evident because all progenitor cells from the BM of Cx32-KO mice showed ~20% decrease in the numbers of CFU-S-13, CFU-S-9 and CFU-GM. Thus, it can be concluded that Cx32 is required for maintaining normal hematopoiesis, specifically during the maturation of hematopoietic stem cells to progenitor cells.

BM transplantation in different combinations of the donor and recipient, which were repopulated with BM cells from either wild-type or Cx32-KO mice, showed a small number of spleen colonies in the groups repopulated with Cx32-KO BM cells (*data not shown*). Interestingly, the colonies derived from the same Cx32-KO BM cells were significantly smaller, regardless of the genotype of the recipients, i.e., wild-type or Cx32-KO mice, presumably owing to the lack of Cx32 expression in the hematopoietic progenitor cells.

Whether Cx32 is also functional in differentiated mature blood cells is, however, questionable despite the observation that the numbers of white blood cells and platelets in the peripheral blood were significantly lower in Cx32-KO than in wild-type mice (Table 1). It is interesting to calculate the probability of Cx32-positive cells on the basis of the ratio of the number of Cx32-positive BM cells to the $Lin^+/c\text{-}kit^-$ fraction, i.e., only 0.0093% of the unfractionated original BM cells (*data not shown*). Because our repeated analysis failed to detect Cx32 expression in mature blood cells, the decreased numbers of white blood cells and platelets in the Cx32-KO mice may reflect the shortage of immature progenitor cell compartments, possibly due to the lack of Cx32 at the level of the stem and progenitor cells.

Flow-cytometric cell cycle analyses of the $Lin^-/c\text{-}kit^+/Sca1^+$, KSL fraction with Hoechst 33342 and the BUUV assay for colony-forming progenitor cells showed that the cell cycle of the hemopoietic stem cell fractions, i.e., the $Lin^-/c\text{-}kit^+/Sca1^+$, KSL or $Lin^-/c\text{-}kit^+$ fraction, seems to be maintained in the quiescence state, thereby maintaining the stemness of the cells, although consequent molecular regulations of these fractions are not yet known.

Acknowledgment The authors thank Dr. K. Sai, Ms. E. Tachihara, Ms. N. Moriyama, Ms. Y. Usami and Ms. M. Uchiyama for excellent technical assistance as well as Ms. N. Kikuchi, Ms. M. Yoshizawa and Ms. M. Hojo for secretarial assistance. Use of FACSAria (BD Biosciences) for flow-cytometric analysis was facilitated by Dr. H. Akiyama and Dr. T. Maitani, Division of Food Sciences, NIHS. This study was supported in part by a Grant-in-Aid for Scientific Research (B 11694334, C 16590329 and C 18510066), the Japan Society for the Promotion of Science Invitation Fellowship for Research in Japan (S01275), the Health Sciences Basic Project and the Integrated Study Project in Drug Innovation Science conducted by the Japan Health Sciences Foundation (KHC1204) and the Ministry of Health, Labour and Welfare (MHLW) Research Fund (H18-Chemistry 001), National Institute of Health Sciences.

References

Bruzzone R, White TW, Paul DL (1996) Connections with connexins: the molecular basis of direct intercellular signaling. Eur J Biochem 238:1–27

Cancelas JA, Koevoet WL, de Koning AE, Mayen AE, Rombouts EJ, Ploemacher RE (2000) Connexin-43 gap junctions are involved in multiconnexin-expressing stromal support of hemopoietic progenitors and stem cells. Blood 96:498–505

Hirabayashi Y, Matsuda M, Aizawa S, Kodama Y, Kanno J, Inoue T (2002) Serial transplantation of p53-deficient hemopoietic progenitor cells to assess their infinite growth potential. Exp Biol Med (Maywood) 227:474–479

Hirabayashi Y, Matsumura T, Matsuda M, Kuramoto K, Motoyoshi K, Yoshida K, Sasaki H, Inoue T (1998) Cell kinetics of hemopoietic colony-forming units in spleen (CFU-S) in young and old mice. Mech Ageing Dev 101:221–231

Krenacs T, Rosendaal M (1998) Connexin43 gap junctions in normal, regenerating, and cultured mouse bone marrow and in human leukemias: their possible involvement in blood formation. Am J Pathol 152:993–1004

Loewenstein WR (1979) Junctional intercellular communication and the control of growth. Biochim Biophys Acta 560:1–65

Montecino-Rodriguez E, Leathers H, Dorshkind K (2000) Expression of connexin 43 (Cx43) is critical for normal hematopoiesis. Blood 96:917–924

Nelles E, Butzler C, Jung D, Temme A, Gabriel HD, Dahl U, Traub O, Stumpel F, Jungermann K, Zielasek J, Toyka KV, Dermietzel R, Willecke K (1996) Defective propagation of signals generated by sympathetic nerve stimulation in the liver of connexin32-deficient mice. Proc Natl Acad Sci USA 93:9565–9570

Ploemacher RE, Mayen AE, De Koning AE, Krenacs T, Rosendaal M (2000) Hematopoiesis: gap junction intercellular communication is likely to be involved in regulation of stroma-dependent proliferation of hemopoietic stem cells. Hematology 5:133–147

Rosendaal M, Gregan A, Green CR (1991) Direct cell-cell communication in the blood-forming system. Tissue Cell 23:457–470

Till JE, McCulloch EA (1961) A direct measurement of the radiation sensitivity of normal mouse bone marrow cells. Radiat Res 14:213–222

Wilson MR, Close TW, Trosko JE (2000) Cell population dynamics (apoptosis, mitosis, and cell-cell communication) during disruption of homeostasis. Exp Cell Res 254:257–268

Yoon BI, Hirabayashi Y, Kawasaki Y, Kodama Y, Kaneko T, Kim DY, Inoue T (2001) Mechanism of action of benzene toxicity: cell cycle suppression in hemopoietic progenitor cells (CFU-GM). Exp Hematol 29:278–285

Yoon BI, Hirabayashi Y, Kawasaki Y, Tsuboi I, Ott T, Kodama Y, Kanno J, Kim DY, Willecke K, Inoue T (2004) Exacerbation of benzene pneumotoxicity in connexin 32 knockout mice: enhanced proliferation of CYP2E1-immunoreactive alveolar epithelial cells. Toxicology 195:19–29